Available online at www.sciencedirect.com

ScienceDirect

Procedia Manufacturing 47 (2020) 623–628

Procedia MANUFACTURING

www.elsevier.com/locate/procedia

23rd International Conference on Material Forming (ESAFORM 2020)

Testing of Formed Gear Wheels at Quasi-Static and Elevated Strain Rates

Till Clausmeyer[a,*], Florian Gutknecht[a], Gregory Gerstein[b], Florian Nürnberger[b]

[a]*Institute of Forming Technology and Lightweight Components, TU Dortmund University, Germany*
[b]*Institut fuer Werkstoffkunde (Materials Science), Leibniz Universität Hannover, Germany*

* Corresponding author. Tel.: +49 231 7558429; fax: +49 231 7552489. *E-mail address:* Till.Clausmeyer@iul.tu-dortmund.de

Abstract

Geared components can be manufactured from sheet metals by sheet-bulk metal forming. One relevant load case in service are overload events, which might induce elevated strain rates. To determine the characteristic hardening and fracture behavior, specimens manufactured from the deep-drawing steel DC04 were tested with strain rates ranging from 0.0001 to 5 s^{-1}. The gear wheels manufactured by sheet-bulk metal forming are tested at crosshead velocities of 0.08 mm/s and 175 mm/s. The tests are analyzed by measuring deformed geometry and hardness. While the tensile tests results show obvious strain-rate dependency, the hardness measurements show no strain-rate depended effect. The analyses are complemented by finite-element-simulations, which assess the homogeneity of deformation and point out the mechanisms of failure. Both coupled and uncoupled ductile damage models are able to predict the critical areas for crack initiation. The coupled damage model has slight advantages regarding deformed shape prediction.

© 2020 The Authors. Published by Elsevier Ltd.
This is an open access article under the CC BY-NC-ND license (https://creativecommons.org/licenses/by-nc-nd/4.0/)
Peer-review under responsibility of the scientific committee of the 23rd International Conference on Material Forming.

Keywords: Sheet-bulk metal forming; Damage; Strain rate; Simulation; Component test; Hardness

1. Introduction

Efficient manufacturing of structural components with integrated functional elements like toothing or carriers requires innovative manufacturing technologies. Sheet-bulk metal forming (SBMF) processes can efficiently produce functional elements directly onto the sheet by controlling the three dimensional material flow, even in the thickness direction [1]. Increasing the thickness only locally when necessary allows using thinner sheets for a component. Thus, the waste of material is significantly reduced and the process chain may be shortened. The technology is accompanied by large local strains and nonlinear strain-paths [2], which may have effect on the components' behavior in overload or crash events. Such an event will generate large strain-rates in the deformation zone. For the user it is of interest how strength, energy absorption and damage initiation or evolution, respectively of components manufactured by SBMF are affected by the elevated strain-rates.

This work exemplary investigates an overload event of a gear wheel manufactured by SBMF process. The load cases incorporate a quasi-static and dynamic scenario. Complementary fatigue testing of gear wheel manufactured by SBMF was performed by Besserer et al. [3]. Section 2 presents the experimental studies of the material behavior. Initially, details of the material and the tensile experiments for calibration of simulation model are given. Afterwards the test rig for the gears is presented, followed by a description of micro-hardness tests, which are used for validation of simulation.

Section 3 describes the simulation setup for assessing strain-rate effects, including the geometric assembly and used material models and identification of material cards.

Finally, in section 4 experiments and simulation are compared. The analysis involves geometric deformation and local entities like plastic strain, hardness and damage.

2351-9789 © 2020 The Authors. Published by Elsevier Ltd.
This is an open access article under the CC BY-NC-ND license (https://creativecommons.org/licenses/by-nc-nd/4.0/)
Peer-review under responsibility of the scientific committee of the 23rd International Conference on Material Forming.
10.1016/j.promfg.2020.04.191

2. Material testing

2.1. Material

The investigated material is a mild deep-drawing steel of grade DC04. Originally, it has a thickness of 2 mm. The local thickness in the toothed area is increased to 3 mm by SBMF.

2.2. Tensile tests

Tensile specimens according to EN-ISO 6892-1 [4] with parallel length of 90 mm are tested on a spindle driven Zwick universal testing machine. A constant speed has been applied, such that the following nominal strain rates are realized: 0.0002 s^{-1}, 0.02 s^{-1} and 0.1 s^{-1}. The material exhibits strain rate-dependent mechanical behavior. The initial flow stresses at the rates of 0.0002, 0.02, 0.1 s^{-1} are 189 MPa, 202 MPa and 213 MPa, respectively. Similar relative increases with respect to the lowest strain are observed for larger strains.

2.3. Split-Hopkinson tests

A Split-Hopkinson Tensile Bar is used for testing at elevated strain-rates. The used incidence and transmitter rod have a length of 2 m each and a diameter of 18 mm. In this study the system is used for investigation of fracture surfaces. Therefore, no force data is recorded. Fig. 1 reveals change of fracture pattern with changing strain-rate.

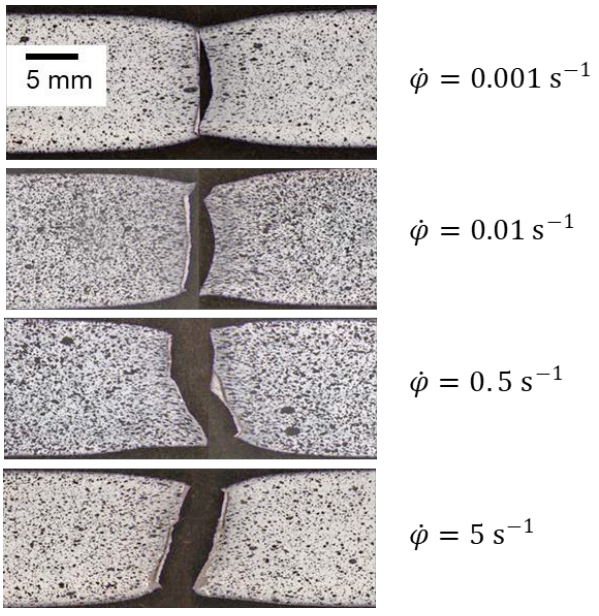

Fig. 1. Tensile Split-Hopkinson specimens after test at different strain rates $\dot{\varphi}$. Fracture pattern changes with increasing strain rate.

2.4. Investigated gear wheel

The manufacturing process of the gears is a two step process involving deep drawing and subsequent upsetting. A detailed description of the process and the simulation of the process is presented in [5]. The geometry of the gear is given in Fig. 2.

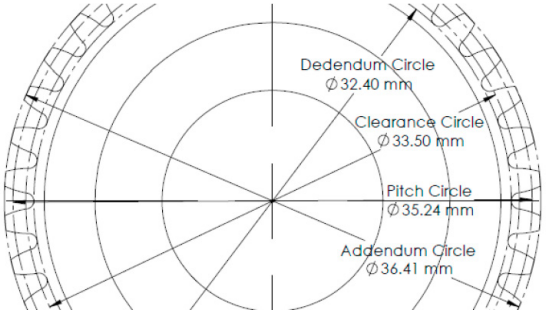

Fig. 2. Geometry of the tested gear wheel.

2.5. Test rig for gear wheels

A test rig to subject single teeth of the gear wheel to plastic deformation is designed for testing on a servo-hydraulic Walter+Bai AG servo-hydraulic universal testing machine with a maximum test load of 25 kN. The maximum cross head velocity is 2500 mm/s. The displacement of the crosshead is approximately 10 mm. The gear wheel is clamped on a free rotating bar (cf. Fig. 3). The gear is connected to a lever with length of 120 mm to transmit the translatory motion of the testing crosshead to a rotation of the gear. The lever is equipped with teeth enclosing the gear teeth so that the load is distributed over several teeth.

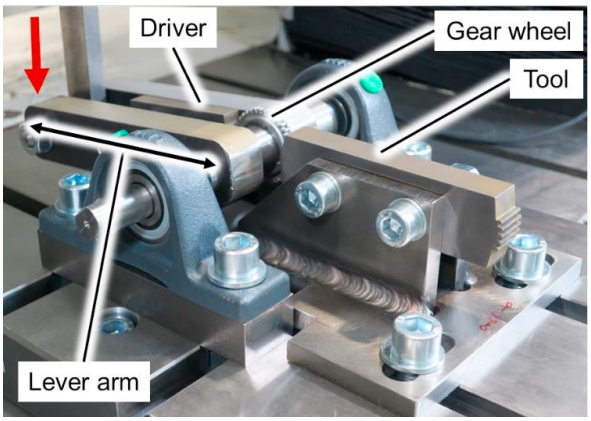

Fig. 3. Test setup mounted in universal testing machine.

With the length of the lever and pitch circle radius of approximately 17.5 mm the teeth experience the circumferential velocity as indicated in Table 1.

Table 1: Testing velocity for gear wheels

Velocity Label	Crosshead velocity	Circumferential velocity
Slow testing velocity	0.08 mm/s	0.012 mm/s
High testing velocity	175 mm/s	25 mm/s

3. Simulation model

3.1. Material modelling

The elasto-plastic behavior is modelled with the Johnson-Cook model:

$$\bar{\sigma} = \left[A + B\left(\bar{\varepsilon}^{\mathrm{pl}}\right)^{n}\right]\left[1 + C\ln\left(\frac{\dot{\bar{\varepsilon}}^{\mathrm{pl}}}{\dot{\varepsilon}_0}\right)\right] \quad (1)$$

Here, A, B and n describe the flow curve at a reference strain rate $\dot{\varepsilon}_0$. The parameters have been fitted by least-square approach (Table 2). The parameter C scales the flow curve for strain rates deviating from $\dot{\varepsilon}_0$. The reference strain rate has been set to $\dot{\varepsilon}_0 = 0.0002\ \mathrm{s}^{-1}$. The other test data at deviating strain rates are equally weighted for determination of C.

Table 2: Elasto-plastic material parameters for investigated DC04.

	A in MPa	B in MPa	n	C
DC04	1	204	0.124	0.013

The agreement of the fitted model with experimental data can be seen in Fig. 4:

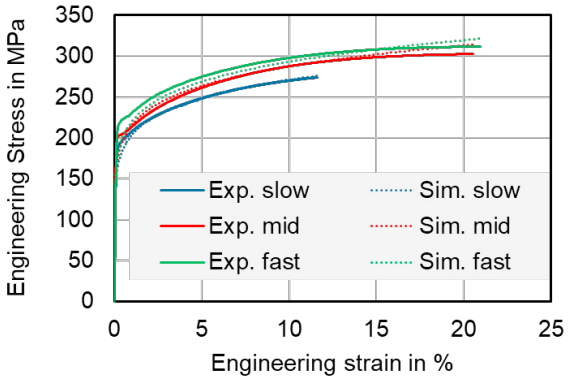

Fig. 4. Experimental and fitted stress-strain curves for different strain-rates. (slow: $\dot{\varphi} = 0.0002\ \mathrm{s}^{-1}$; mid: $\dot{\varphi} = 0.02\ \mathrm{s}^{-1}$; fast: $\dot{\varphi} = 0.1\ \mathrm{s}^{-1}$;

The damage is modelled with two different approaches. A coupled approach is realized with the Abaqus ductile damage model (ADD) [6]. Its concept relies on a damage initiation strain $\varepsilon_{\mathrm{init}}(\eta)$ and an evolution law, which can account for stiffness and strength degradation.

Here, η is the triaxiality $\eta = \sigma_{\mathrm{hyd}}/\sigma_{\mathrm{eqv}}$, with σ_{hyd} and σ_{eqv} the hydrostatic and equivalent stress, respectively.

The evolution of damage follows a linear law until the specified fracture displacement $u_{\mathrm{f}}^{\mathrm{pl}}$ is reached. The concept of a fracture displacement alleviates the mesh dependency observed when using material models with degrading stiffness or strength. Previously conducted Nakajima tests [7] are used for the determination of damage initiation strain $\varepsilon_{\mathrm{init}}(\eta)$ (see Table 3). The onset of necking is assumed mark the beginning of damage evolution. From the known strain state a corresponding triaxiality can be calculated [8]. The fracture displacement $u_{\mathrm{f}}^{\mathrm{pl}}$ is determined by:

$$u_{\mathrm{f}}^{\mathrm{pl}} = L\,\varepsilon_{\mathrm{f}}^{\mathrm{pl}} \quad (2)$$

where L is the characteristic element length L = 0.05 mm and $\varepsilon_{\mathrm{f}}^{\mathrm{pl}}$ is chosen as the macroscopic strain in uniaxial tension experiments between ultimate strength and final rupture.

Table 3: Damage material parameters for investigated steels.

	$\varepsilon_{\mathrm{init}}(\eta)$					$u_{\mathrm{f}}^{\mathrm{pl}}$
η	-1.0	-0.33	0	0.33	1	
DC04	10	5	2	0.5	0.5	0.08

The second approach is a version of the Lemaitre model with enhancement for low triaxiality. The model parameter may be identified with fewer experiments. Besides, it is of interest to compare coupled and uncoupled approach in use case scenario. The evolution of damage D is given by:

$$\dot{D} = \dot{\gamma}\left\langle\frac{Y - Y_0}{S}\right\rangle^{\delta}\frac{1}{[1 - D]^{\beta}} \quad (3)$$

Here, $\dot{\gamma}$ is the plastic increment and S, Y_0, δ, β are parameters of the model. The driving force Y is defined by:

$$Y = \frac{1+\nu}{2\,E}\left[\frac{\langle\sigma\rangle_{\mathrm{ij}}\langle\sigma\rangle_{\mathrm{ij}}}{(1-D)^2} + h\frac{\langle-\sigma\rangle_{\mathrm{ij}}\langle-\sigma\rangle_{\mathrm{ij}}}{(1-hD)^2}\right] - \frac{\nu}{2\,E}\left[\frac{\langle\sigma_{\mathrm{kk}}\rangle^2}{(1-D)^2} + h\frac{\langle-\sigma_{\mathrm{kk}}\rangle^2}{(1-hD)^2}\right] \quad (4)$$

Herein, the parameter h weighs the evolution of damage under compressive hydrostatic stress. The model is used in an uncoupled version [9]. Thus, the damage does not affect neither strength nor stiffness. The parameters have been identified in a previous investigation [9].

Earlier works have shown significant prestrain in the zone of the formed gears [10]. The entire forming zone exhibits strains of approximately 1.0. Only in the vicinity of the tooth surface there is a larger strain. Due to different mesh size in forming and testing simulation the prestrain in the current simulations is approximated as 1.0 with uniform distribution.

Furthermore, the damage level for current simulations is set to zero. This is justified, since Isik et al. [9] showed that there is little damage evolution in the compression-dominated manufacturing process. It also enables a comparison of the current ADD model and the damage models used in forming simulations.

3.2. Model setup for gear wheel tests

The simulation is performed with Abaqus 2019 using implicit dynamic time integration. The used elements are 8-node linear hexahedra with reduced integration and hourglass control (C3D8R). The contact between gear and tool is realized with a surface-to-surface algorithm. Penetration is avoided by penalty method. The Coulomb friction coefficient is set to μ=0.1. A convergence study proved that discretization with elements of 0.05 mm edge length is sufficient. In addition, the contact algorithm has negligible influence on the predicted results.

In an initial step the “complete” test rig assembly is modeled including driver, single tooth tool and entire gear wheel (cf. Fig. 5).

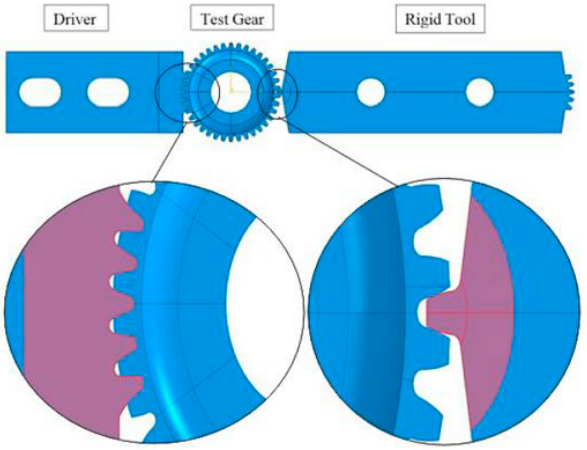

Fig. 5. Assembly of the "complete" model. Driver and tools are modelled as rigid parts.

The analysis of the above setup revealed that the deformation in the gear highly concentrated in a single tooth region. Therefore, in the following investigations the model is reduced to a 47.4° section of the entire gear (Fig. 6).

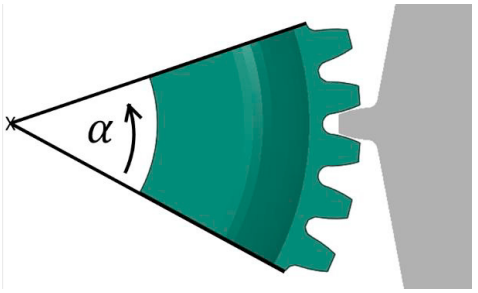

Fig. 6. Assembly of reduced model. The gear rotates in upward direction.

4. Results and Discussion

4.1. Experimental results

All specimens tested in the test rig exhibit a similar deformation behavior (Fig. 7 and Fig. 8). There is a pronounced shear deformation at a distance equivalent to about approximately half of the distance between the tooth base and the tooth head. This leads to tilting of the upper half of the tooth in the direction of the applied rotational motion. Due to the severe plastic deformation, the moving tooth in contact with the specimen forms a plateau, marked by straight region. The length of this shear plateau is a measure of the experienced plastic deformation and resistance against damage of the material. During the testing in the test rig, the substantial plastic strain leads to a pronounced crack on the side of the specimen tested at velocity of 0.08 mm/s, which is in contact with the moving tooth. There is also an incipient crack at the base of the tooth at the opposite side. There is considerable deformation with a region where the side of the tooth and material from the base come into contact. The width of the shear plateau and the width of the sheared zone are chosen as geometric measures to quantify the deformation, the effect of damage and the strain rate. The shear plateau width is 624 µm for the gear tested at 0.08 mm/s and 652 µm for the gear tested at 175 mm/s. Correspondingly, the width of the sheared zone are 1062 µm and 1097 µm for the gears tested at 0.08 mm/s and 175 mm/s, respectively. This means that the width of the sheared plateau increases by 4.5% when the test velocity is increased from 0.08 mm/s to 175 mm/s.

The influence of strain-rate dependent local deformation on the deformed tooth is assessed by micro-hardness test. Tests are performed according to Qness Standard microhardness test with a penetration force of 0.05 kPond and duration of 11 s. The measurement spot lies in the deformed zone (cf. Fig. 7). The determined hardness values is the average of 9 single measurements performed for the specific measurement spot.

The experiments with the faster testing velocity have a hardness of 224 HV and the experiments with the slower testing velocity have a hardness of 225 HV. For both experiments, the accuracy of the hardness measurement is +/- 20 HV. As reference, the untested gear wheel manufactured by SBMF has a hardness 200 HV +/- 10 HV. According to the experiments the strength of the most severely deformed region should not be affected by the different strain rate.

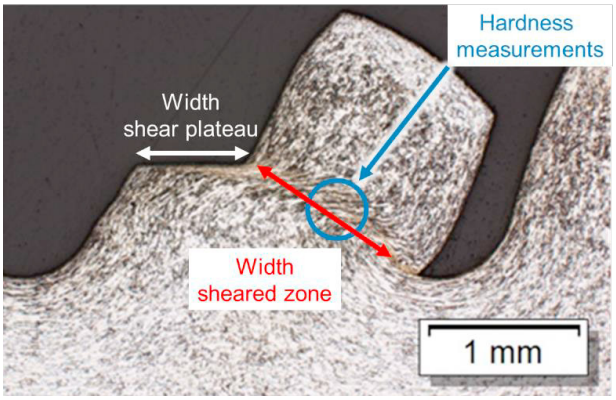

Fig. 7. Measures for geometric deformation and location of spot for micro-hardness measurements, here representatively shown for a gear wheel tested at 0.08 mm/s.

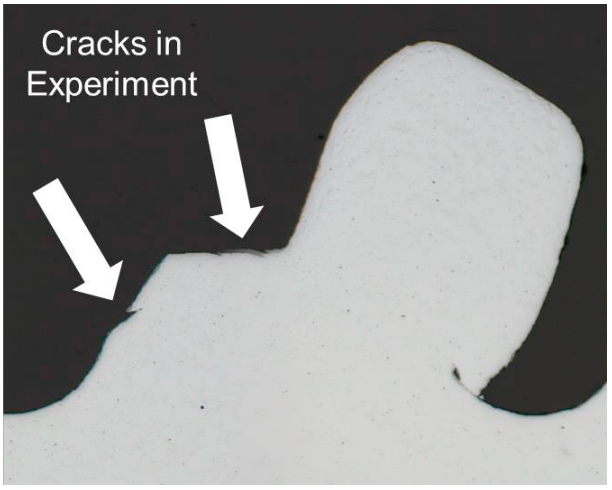

Fig. 8. Cracks observed in experiment for gear wheel tested at 0.08 mm/s

4.2. Simulation results

Both experiments and simulations show similar trends in the deformation of the tooth. With elevated testing speed, the width of the sheared zone increases by 3.3% for experiments and by 3.0% for simulation. In addition, the width of the sheared plateau increases similarly. In experiments the increase was 4.5% and in simulation it increased by 3.4% (cf. Fig. 7).

Interestingly, those trends are only valid for the ADD. Simulations with Lemaitre were not able to capture these trends. It is assumed that the coupling of the damage to the strength and the stiffness in the ADD are responsible for the differences. Yet, both damage models predict similar damage distribution. The maximum values occur in the transition zone from the shear plateau to the side of the tooth in contact with the moving tooth. The head of the moving gear severely deforms the tested gear wheel in this region. The analysis of the stress triaxiality reveals that this region is governed by tension-dominated stress states with triaxialities > 0.4. This tendency is observed for the simulations with the testing speed of 0.08 mm/s and 175 mm/s. The predicted damage distribution is reasonable for both damage models and coincides with cracks spotted on the deformed tooth (Fig. 8 and Fig. 9).

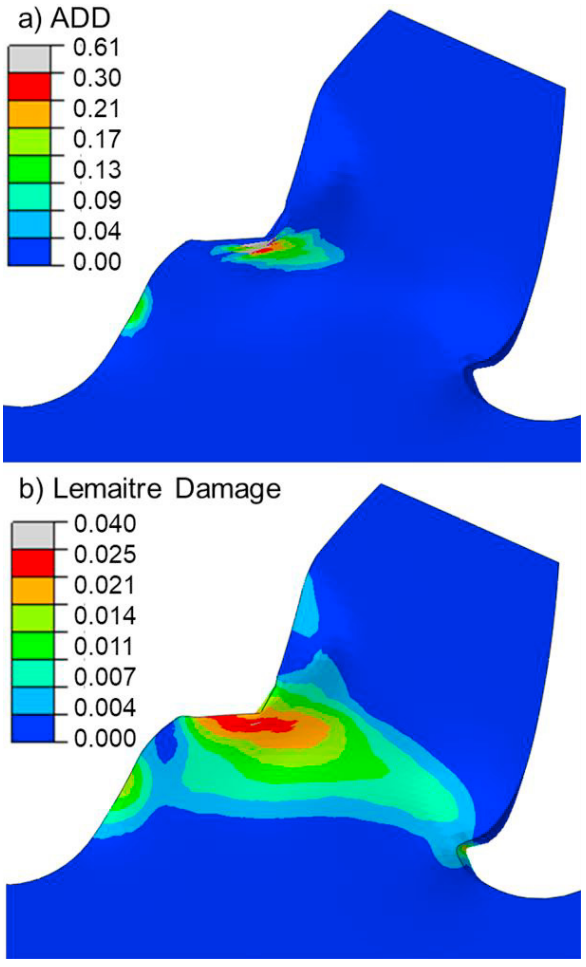

Fig. 9. Damage prediction by ADD model (a) and Lemaitre model (b), respectively. All results for slow testing velocity.

A strength of the Lemaitre model is the physically motivated correlation of its damage value to the void area fraction. Thus, the damage value is significantly below the value predicted by ADD model (0.025 vs. 0.3, respectively). For instance relatively low void area fractions were determined in [11].

The plastic strain in the deformation zone is almost independent of the testing speed or the applied damage model (Fig. 10). The path is plotted along the sheared zone, starting at the end of the shear plateau (cf. Fig. 7).

This is in good correlation to the hardness measured in the deformed area (Fig. 10). Slight deviations can be found for the ADD. This is due to the accumulation of damage in this region (cf. Fig. 11). The reduction of stiffness and strength increases slightly with the accumulation of plastic strain for the coupled model.

Finally, the testing speed affects the evolution of damage. Higher strain-rate results in higher damage levels for both Lemaitre model and ductile damage model.

For analysis of this effect, simulations have been repeated with a deactivated strain-rate dependent term, such that only inertia effects take place.

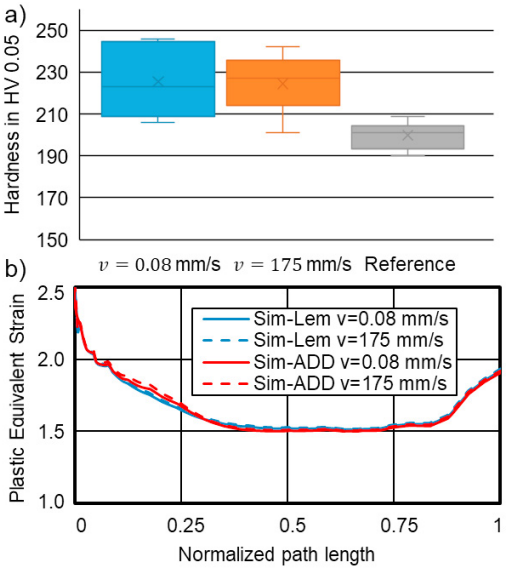

Fig. 10. a): Hardness in the deformed zones for slow and fast testing velocity. 'Reference' refers to an untested gear wheel; b): Model predictions of plastic equivalent strain models along the deformation zone for both testing velocities and both damage. (ADD: Abaqus ductile damage model, Lem: Lemaitre damage model)

In that case no difference between slow and fast testing could be observed. Thus, the increased damage evolution is triggered by the strain rate sensitivity of the material and not by inertia effects.

In previous analysis of machined gear wheels from steel, the teeth failed at the tooth base [12]. The used testing stand was differently designed such that the contact point of the tooth was closer to the tooth base. In the current investigation it was not possible to shift the contact point closer to the tooth base.

5. Conclusion

Gear wheels manufactured by SBMF have been tested in a specialized testing rig for an overload event. Tests have been conducted at low and elevated velocity. The geometry of the deformed gear wheels as well as their hardness have been investigated. It has been found that the hardness is not affected by the testing velocity.

Simulations to increase the insight have accompanied the investigations. The plasticity was modelled as strain-rate dependent with data from tensile tests. The damage has been investigated by both an uncoupled Lemaitre model, and the fully coupled ADD model. It has been found that both damage models produce reasonable results. The coupled model has slight advantages concerning the prediction of shape deviation.

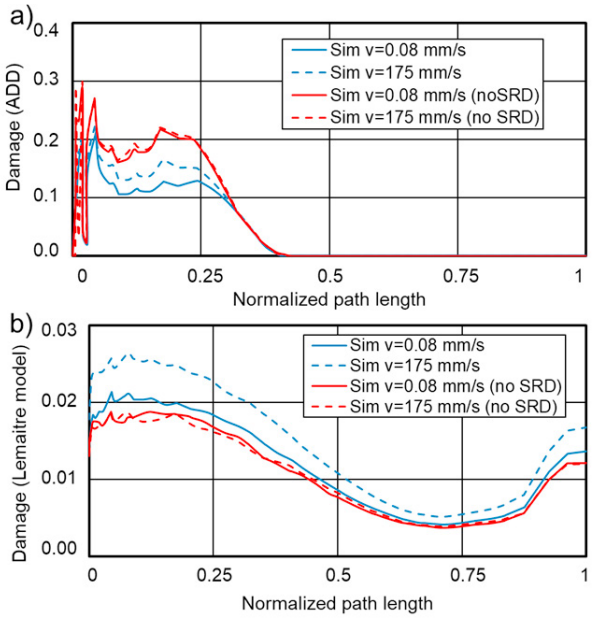

Fig. 11. Damage prediction by ADD model (upper) and Lemaitre model (lower), respectively. Path plot along the sheared zone starting at the end of the shear plateau. (noSRD: deactivated strain rate dependency in plasticity model)

Acknowledgements

The authors gratefully acknowledge funding by the German Research Foundation (DFG) within the scope of the Transregional Collaborative Research Centre on sheet-bulk metal forming (SFB/TR73) in the subproject C4 “Analysis of load history dependent evolution of damage and microstructure for the numerical design of sheet-bulk metal forming processes” (Project number: 116969364).

IFUM (Institute of Forming Technology and Machines, subproject A7) is thanked for providing the formed gear wheels.

Mr. Faizan Tariq (former student at IUL) is thanked for his initial work on the simulation model.

References

[1] Merklein M, Hagenah H. Introduction to sheet-bulk metal forming. Prod. Eng. Res. Devel. 2016;10(1):1–3.

[2] Mori K, Abe Y, Osakada K, Hiramatsu S. Plate forging of tailored blanks having local thickening for deep drawing of square cups. J. Mater. Process. Tech. 2011;211(10):1569–74.

[3] Besserer H-B, Hildenbrand P, Gerstein G, Rodman D, Nürnberger F, Merklein M et al. Ductile Damage and Fatigue Behavior of Semi-Finished Tailored Blanks for Sheet-Bulk Metal Forming Processes. J. of Materi Eng and Perform 2016;25(3):1136–42.

[4] EN-ISO 6892-1. Metallic materials - Tensile testing: Part 1: Method of test at room temperature. 2017th ed;77.040.10(6892-1).

[5] Behrens BA, Bouguecha A, Vucetic M, Hübner S, Rosenbusch D, Koch S. Numerical and Experimental Investigations of Multistage Sheet-Bulk Metal Forming Process with Compound Press Tools. Key. Eng. Mat. (Key Engineering Materials) 2015;651-653:1153–8.

[6] Dassault Systèmes. SIMULIA User Assistance 2019: Abaqus; Available from: https://help.3ds.com.

[7] Isik K. Modelling and characterization of damage and fracture in sheet-bulk metal forming. 1st ed. Herzogenrath: Shaker; 2018.

[8] Marciniak Z, Duncan JL, Hu SJ. Mechanics of Sheet Metal Forming. Butterworth-Heinemann; 2002.

[9] Isik K, Gerstein G, Schneider T, Schulte R, Rosenbusch D, Clausmeyer T et al. Investigations of ductile damage during the process chains of toothed functional components manufactured by sheet-bulk metal forming. Prod. Eng. Res. Devel. 2016;10(1):5–15.

[10] Behrens BA, Vucetic M, Hübner S, Koch S, Denkena B, Grove T, Lucas H, Tillmann W, Stangier D, Hausotte T, Loderer A. Werkzeugoberflächen mittels schwingungsüberlagertem Flachstauchversuch für die Blechmassivumformung. In: Tekkaya AE, Liewald M, Merklein M, Behrens B-A, editors. 18. Workshop Simulation in der Umformtechnik & 3. Industriekolloquium des SFB/TR73: Dortmund, 26.-27. February 2015. Aachen: Shaker; 2015.

[11] Isik K, Gerstein G, Clausmeyer T, Nürnberger F, Tekkaya AE, Maier HJ. Evaluation of Void Nucleation and Development during Plastic Deformation of Dual-Phase Steel DP600. steel research international 2016;87(12):1583–91.

[12] Boiadjiev I, Witzig J, Tobie T, Stahl K. Tooth flank fracture – basic principles and calculation model for a sub surface initiated fatigue failure mode of case hardened gears. In: International gear conference 2014: 26th-28th August 2014, Lyon Villeurbanne, France. Cambridge: Woodhead Publishing an imprint of Elsevier; 2014, p. 670–680.

'